REPORT 1302

ON PANEL FLUTTER AND DIVERGENCE OF INFINITELY LONG UNSTIFFENED AND RING-STIFFENED THIN-WALLED CIRCULAR CYLINDERS [1]

By Robert W. Leonard and John M. Hedgepeth

SUMMARY

A preliminary theoretical investigation of the panel flutter and divergence of infinitely long, unstiffened and ring-stiffened thin-walled circular cylinders is described. Linearized unsteady potential-flow theory is utilized in conjunction with Donnell's cylinder theory to obtain equilibrium equations for panel flutter. Where necessary, a simplified version of Flügge's cylinder theory is used to obtain greater accuracy. By applying Nyquist diagram techniques, analytical criteria for the location of stability boundaries are derived. A limited number of computed results are presented.

INTRODUCTION

Although considerable effort has been expended in studying the flutter and divergence of thin, flat panels exposed to an airstream (see, for example, refs. 1 to 9), little is known of the importance of similar aeroelastic phenomena in the design of thin-walled cylindrical missile bodies or of other aircraft components where thin, curved panels are used. The purpose of this report is to describe a preliminary theoretical investigation of the aeroelastic stability of such configurations. Analytical criteria for the determination of panel-flutter and panel-divergence boundaries for infinitely long, unstiffened and ring-stiffened thin-walled circular cylinders are presented along with a limited number of computed results.

SYMBOLS

a	distance between ring stiffeners
a_m	amplitude of mth term in expansion for lateral motion of ring-stiffened cylinder
b	dummy variable
c	speed of sound in air
c_i	speed of sound in fluid inside cylinder
c_s	speed of sound in cylinder material, $\sqrt{\frac{E}{\rho_s}}$
D	plate flexural stiffness per unit length, $\frac{Eh^3}{12(1-\mu^2)}$
E	Young's modulus
e	base of natural system of logarithms
F,F_i	outside and inside air-force functions defined by equations (5) and (6), respectively
G,G_i	outside and inside air-force functions for vibrating ring (see eqs. (34) and (35), respectively)
$H_n^{(1)},H_n^{(2)}$	Hankel functions of first and second kind, respectively, of order n
h	thickness of cylinder wall
Im	imaginary part
I_n	modified Bessel function of first kind of order n
$i=\sqrt{-1}$	
J_n	Bessel function of first kind of order n
j	integer
K_n	modified Bessel function of second kind of order n
k	dimensionless frequency of harmonic vibration, $\frac{\omega}{\nu c}$ for unstiffened cylinder and $\frac{\omega a}{\pi c}$ for ring-stiffened cylinder
k_j	resonant frequencies of internal air-force function for unstiffened cylinder (see eq. (22))
L	function defined by equation (8)
$\bar{L}$	function defined by equation (9)
l	outward lift force on cylinder wall
$\bar{l}$	amplitude of harmonically varying outward lift force for unstiffened cylinder
l_m	amplitude of mth term in expansion for outward lift force for stiffened cylinder
M	Mach number of flow along vibrating cylinder
M_1	Mach number of external or internal flow along stationary cylinder
m	integer, number of longitudinal half-waves in each bay of ring-stiffened cylinder
N	function defined by equation (44)
n	integer, number of full waves around circumference of cylinder
P_0,P_1	forces exerted on cylinder wall by ring stiffeners
$\bar{P}_0,\bar{P}_1$	amplitudes of harmonically varying reaction forces exerted by ring stiffeners
R	radius of cylinder
Re	real part
r	radial coordinate
t	time
w	lateral deflection of cylinder wall, positive outward

[1] Supersedes NACA Technical Note 3638 by Robert W. Leonard and John M. Hedgepeth, 1956.

$\bar{w}$ amplitude of lateral motion of cylinder wall for unstiffened cylinder
x longitudinal coordinate for vibrating cylinder
x_1 longitudinal coordinate for stationary cylinder
z argument of Bessel functions for supersonic relative flow, $|\bar{\nu}|\sqrt{\xi^2-1}$ for unstiffened cylinder and $|m|\alpha\sqrt{\xi^2-1}$ for stiffened cylinder
α aspect-ratio parameter, $R\pi/a$
β_m function defined after equation (39)
$\delta(x)$ Dirac delta function, $\delta(x)=0$ for $x\neq 0$; $\int_{-\infty}^{\infty}\delta(x)dx=1$
ϵ damping coefficient
ζ argument of Bessel functions for subsonic relative flow, $|\bar{\nu}|\sqrt{1-\xi^2}$ for unstiffened cylinder and $|m|\alpha\sqrt{1-\xi^2}$ for stiffened cylinder
θ angular circumferential coordinate
μ Poisson's ratio
ν wave number of longitudinal waves in unstiffened cylinder
$\bar{\nu}$ dimensionless wave number, $R\nu$
ξ dummy variable
ρ mass density of air
ρ_l mass density of fluid inside cylinder
ρ_s mass density of cylinder material
σ_θ,σ_x midplane stresses in circumferential and longitudinal directions, positive in tension
$\bar{\sigma}_\theta,\bar{\sigma}_x$ dimensionless midplane stresses, σ_θ/E and σ_x/E, respectively
Ω parameter defined after equation (8)
Ω_m parameter defined after equation (39)
ω frequency of harmonic vibration
∇^4 operator, $\left(\frac{\partial^2}{\partial x^2}+\frac{1}{R^2}\frac{\partial^2}{\partial\theta^2}\right)^2$
∇^{-4} inverse of operator ∇^4

Subscripts:
cr critical value
min minimum value
max maximum value

Primes are used to indicate differentiation with respect to complete argument. Subscript notation is used to denote partial differentiation.

METHOD OF APPROACH

The configuration under consideration consists of a thin-walled unstiffened or ring-stiffened circular cylinder extending to infinity in the positive and negative x-directions. (See fig. 1.) The cylinder is filled with a stationary fluid and is surrounded by air flowing in the positive x-direction at a Mach number M. The effects of midplane tensile stresses in both the circumferential and longitudinal directions and of a small amount of structural damping are taken into account.

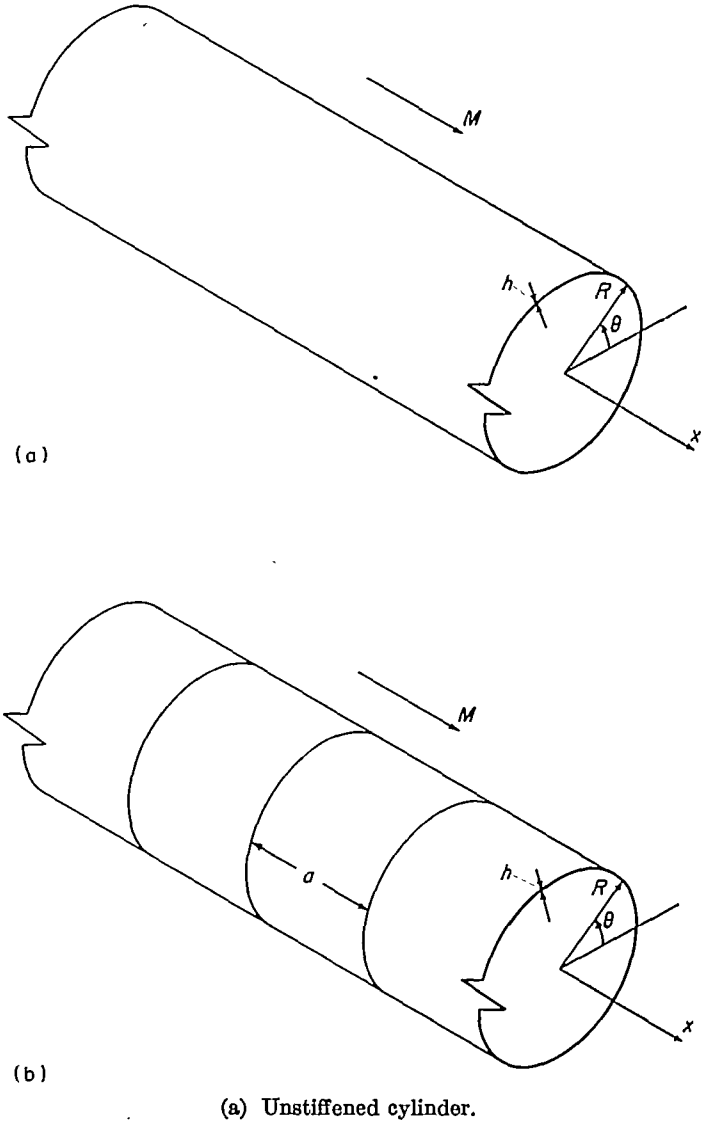

(a) Unstiffened cylinder.
(b) Ring-stiffened cylinder.

FIGURE 1.—Infinitely long, thin-walled circular cylinder with air flow outside and stationary fluid inside.

For simplicity in the analysis, it is assumed that the deformations of the cylinder walls can in most cases be adequately described by Donnell's differential equation. (See ref. 10.) It is kept in mind, however, that the validity of Donnell's theory is limited to cases in which there are a large number of circumferential waves; where this condition is violated, a simplified version of Flügge's cylinder theory (see refs. 11 and 12) is employed to improve the accuracy of the results.

The problem to be considered is the determination of those combinations of the parameters characterizing the cylinder and its environment that correspond to the boundary between states of stable and unstable motion. For the purposes of this report, a system is considered stable if its

motion is either damped or purely sinusoidal; only timewise divergent motion is considered to be unstable. In order to determine the stability boundary itself, attention can be restricted to simple harmonic motion. However, such simple-harmonic-motion analyses often yield a multiplicity of boundaries, and it is necessary to derive equilibrium conditions for divergent oscillatory motions in order to determine the degree of instability in regions separated by the various boundaries and, thus, to identify the primary stability boundary.

In line with the foregoing discussion, the method of approach is first to derive the equilibrium conditions for sinusoidal motion. These conditions are then extended to apply to divergent motion by means of analytic continuation. A Nyquist diagram technique is used to determine states of stability and stability boundaries.

UNSTIFFENED CYLINDER

DERIVATION OF EQUATIONS

It is assumed herein that the cylinder wall may deform into any number of sinusoidal waves around its circumference and into sinusoidal waves of any wave length and constant amplitude along its length and, further, that the motion is simple harmonic in time; spacewise divergent motion (motion increasing in amplitude along the cylinder) is specifically excluded. Thus, the lateral deflection of the cylinder wall may be written

$$\begin{aligned} w(x,\theta,t)&=\mathrm{Re}(\overline{w}e^{-i\nu x}e^{i\omega t}\cos n\theta)\\ &=\mathrm{Re}\left[\overline{w}e^{-i\nu\left(x-\frac{\omega}{\nu}t\right)}\cos n\theta\right] \qquad (n=2,3,4,\ldots) \end{aligned} \tag{1}$$

where $\overline{w}$ is the complex amplitude of the motion, ν is the real wave number of the longitudinal waves, n is the number of full waves around the circumference, and ω is the frequency of oscillation. This assumed deflection shape will be the basis for the determination of the air forces exerted on the cylinder, the equilibrium condition, and, through it, the criteria for flutter. Note that $n=0$ and $n=1$ have been specifically excluded from consideration in this panel-flutter analysis because neither of these two motions involves panel action. The first value $n=0$ represents pure dilation or contraction of the cross section; the second value $n=1$ merely represents a rigid-body translation of the cross section.

Air forces.—The air forces exerted on an infinite cylinder vibrating harmonically in still air have been reported in the literature. (See, for example, ref. 13.) Although some of these results can be applied to the present problem of determining the forces exerted on an oscillating cylinder in moving air, it is convenient to derive this result directly. The unsteady-flow problem can be reduced to a steady-flow problem by means of a moving coordinate system in a manner similar to that of reference 7.

Accordingly, the perturbation pressures exerted by a steady external or internal flow of Mach number M_1 on a stationary cylinder deformed in the shape

$$w=\mathrm{Re}(\overline{w}e^{-i\nu x_1}\cos n\theta) \tag{2}$$

have been determined in appendix A. The assumed deformation (eq. (1)) has the form of a wave traveling in the positive x-direction with velocity ω/ν; hence, the flow of Mach number M outside the vibrating cylinder is equivalent to a flow of Mach number $M-\omega/\nu c$ outside the stationary cylinder plus a flow of Mach number $-\omega/\nu c_i$ inside the stationary cylinder. Thus, by making the appropriate substitutions, the steady-flow results of appendix A are readily combined to give, for the outward air force exerted on a vibrating cylinder,

$$l(x,\theta,t)=R\nu^2\mathrm{Re}\left[\overline{l}\overline{w}e^{-i\nu\left(x-\frac{\omega}{\nu}t\right)}\cos n\theta\right] \tag{3}$$

where

$$\overline{l}=-\rho c^2F(M-k,\overline{\nu},n)+\rho_i c_i^2F_i\left(\frac{c}{c_i}k,\overline{\nu},n\right) \tag{4}$$

In equation (4),

$$\left.\begin{aligned} F(\xi,b,n)&=\xi^2\frac{K_n(\zeta)}{\zeta K_n'(\zeta)} && (|\xi|<1)\\ &=\xi^2\frac{H_n^{(j)}(z)}{zH_n^{(j)\prime}(z)} \quad \left(j=\begin{cases}1 \text{ for } b\xi>0\\ 2 \text{ for } b\xi<0\end{cases}\right) && (|\xi|>1) \end{aligned}\right\} \tag{5}$$

$$\left.\begin{aligned} F_i(\xi,b,n)&=\xi^2\frac{I_n(\zeta)}{\zeta I_n'(\zeta)} && (|\xi|<1)\\ &=\xi^2\frac{J_n(z)}{zJ_n'(z)} && (|\xi|>1) \end{aligned}\right\} \tag{6}$$

with

$$\zeta=|b|\sqrt{1-\xi^2}$$

$$z=|b|\sqrt{\xi^2-1}$$

In equations (5) and (6), J_n is the Bessel function of the first kind, $H_n^{(j)}$ is the Hankel function of the first or second kind, and I_n and K_n are modified Bessel functions of the first and second kind, respectively. (See, for example, refs. 14 and 15.) The primed quantity in the denominator of each function is the derivative with respect to the entire argument. Note that a dimensionless frequency $k=\omega/\nu c$ and a dimensionless wave number $\overline{\nu}=R\nu$ have been introduced in equation (4).

Equilibrium condition.—Donnell's equation for the equilibrium of thin, cylindrical shells (ref. 10) may be written in the modified form (see, for example, ref. 16)

$$D\left[\nabla^4w+\frac{1}{R^4}\frac{12(1-\mu^2)}{\left(\frac{h}{R}\right)^2}\nabla^{-4}w_{xxxx}\right]-h\left(\sigma_xw_{xx}+\frac{\sigma_\theta}{R^2}w_{\theta\theta}\right)+\rho_shw_{tt}=l \tag{7}$$

where the subscripts x, θ, and t on w indicate differentiation with respect to these variables. The operators ∇^4 and ∇^{-4} are defined by

$$\nabla^4=\left(\frac{\partial^2}{\partial x^2}+\frac{1}{R^2}\frac{\partial^2}{\partial\theta^2}\right)^2$$

and

$$\nabla^{-4}\nabla^4=\nabla^4\nabla^{-4}=1$$

Substitution of w and l from equations (1) and (3) into equation (7) gives

$$D\left[\left(\nu^2+\frac{n^2}{R^2}\right)^2+\frac{1}{R^4}\frac{12(1-\mu^2)}{\left(\frac{h}{R}\right)^2}\frac{\nu^4}{\left(\nu^2+\frac{n^2}{R^2}\right)^2}\right]+h\left(\nu^2\sigma_x+\frac{n^2}{R^2}\sigma_\theta\right)-\rho_s h\omega^2-R\nu^2\bar{l}=0$$

as the condition for equilibrium of the motion of the cylinder wall in the presence of the moving air outside and the stationary fluid inside the cylinder. Written in terms of pertinent nondimensional parameters, this expression becomes

$$L\equiv\frac{\rho_s}{\rho}\frac{h}{R}(k^2-\Omega^2)+\frac{\rho_t}{\rho}\left(\frac{c_t}{c}\right)^2F_t\left(\frac{c}{c_t}k,\bar{\nu},n\right)-F(M-k,\bar{\nu},n)-i\frac{\bar{\nu}}{|\bar{\nu}|}\epsilon k=0 \tag{8}$$

where

$$\Omega=\frac{\frac{c_s}{c}\frac{h}{R}}{\sqrt{12(1-\mu^2)}}\sqrt{\bar{\nu}^2\left(1+\frac{n^2}{\bar{\nu}^2}\right)^2+\frac{12(1-\mu^2)}{\left(\frac{h}{R}\right)^2}\left[\frac{1}{\bar{\nu}^2\left(1+\frac{n^2}{\bar{\nu}^2}\right)^2}+\bar{\sigma}_x+\frac{n^2}{\bar{\nu}^2}\bar{\sigma}_\theta\right]}$$

In the preceding definition, $\bar{\sigma}=\sigma/E$, and $c_s=\sqrt{E/\rho_s}$ is the speed of sound in the cylinder material. Note that, in equation (8), an additional term $-i\frac{\bar{\nu}}{|\bar{\nu}|}\epsilon k$ has been added in order to include qualitatively the effects of structural damping of the Sezawa (viscous) type. The damping coefficient ϵ is actually related to the parameters of the system in a rather complicated fashion but is always positive. A precise definition of ϵ is not necessary because, in the following derivation, it is considered to be a vanishingly small, positive quantity.

EXTENSION OF EQUILIBRIUM EQUATION TO DIVERGENT MOTION

The flutter equation (eq. (8)) has been derived for sinusoidal motion. As has been pointed out, an extension to divergent motion (of the form of eq. (1) with ω a complex number having a negative imaginary part) is necessary. This requires the analytic continuation of equation (8) into the complex k-plane. The only terms in equation (8) for which this continuation is not trivial are the air-force functions F and F_t. The analytic continuations of these functions are presented and discussed in appendix B. These functions are analytic throughout the half-plane corresponding to divergent motion and approach the values given by equations (5) and (6) as k becomes real. That the analytic extension of equation (8) into the lower half of the ω-plane is indeed the equilibrium equation for divergent motion of the cylinder can be rigorously shown by the application of Fourier transform analysis.

STABILITY DETERMINATION BY USE OF NYQUIST DIAGRAMS

In order to determine the stability states of the structure whose behavior is governed by equation (8), it is expedient to examine the variation of the function L in the L-plane as k traverses, in the clockwise direction, a curve enclosing that portion of the k-plane corresponding to divergent motion of the cylinder (the lower half-plane for positive values of $\bar{\nu}$ or the upper half-plane for negative values of $\bar{\nu}$). This, of course, is the well-known Nyquist diagram. (See, for example, ref. 7.) The number of resulting clockwise encirclements of the origin in the L-plane is equal to the number of zeros of L minus the number of poles of L enclosed by the curve traversed in the k-plane. Poles of L do not occur in the unstable half-plane since the functions comprising L are analytic everywhere in that region. (It should be noted that, in all instances, the real k-axis is excluded from the unstable half-plane.) Therefore, the Nyquist diagram gives directly the number of roots of equation (8) for which the frequency of oscillation has a negative imaginary part; in other words, it gives directly the number of modes of unstable motion.

With regard to the practical application of the Nyquist diagrams in the present case, it should be pointed out that actual computation of successive values of L is unnecessary; that is, through careful examination of the nature of the functions comprising L, it is possible to construct approximate diagrams correct in all essential features and to see clearly the conditions under which critical changes (corresponding to flutter boundaries) occur. Further, it is only necessary to consider positive values of $\bar{\nu}$ because, if $\bar{\nu}$ is replaced by its negative and k by its conjugate, then L is replaced by its conjugate; therefore, no new flutter boundaries would result from the negative values of $\bar{\nu}$.

ANALYSIS OF EMPTY CYLINDER

Flutter criteria.—If the cylinder is assumed to be empty ($\rho_t=0$), equation (8) reduces to

$$\bar{L}\equiv\frac{\rho_s}{\rho}\frac{h}{R}(k^2-\Omega^2)-F(M-k,\bar{\nu},n)-i\frac{\bar{\nu}}{|\bar{\nu}|}\epsilon k=0 \tag{9}$$

Let the damping coefficient ϵ be very small but positive. With this restriction, the functions comprising $\bar{L}$ (for $\bar{\nu}>0$) vary with k in the manner shown in figure 2. Note that the inclusion of the infinitesimal damping is influential only in the range $M-1<k<M+1$ where $\mathrm{Im}(-F)=0$; elsewhere, $\mathrm{Im}(-F)$ is large in comparison with the damping term. In the range $M-1<k<M+1$, the damping makes $\mathrm{Im}(\bar{L})$ negative for positive k and positive for negative k. Hence, for subsonic flow (fig. 2(a)), the damping insures that $\mathrm{Im}(\bar{L})=0$ only at $k=0$; for supersonic flow (fig. 2(b)), it permits $\mathrm{Im}(\bar{L})=0$ only at $k=M-1$ (in the limit as $\epsilon\to0$). The significance of this will be made apparent by considering the variation of $\bar{L}$ as k traverses the path shown in figure 3 (with the other parameters held constant).

First, consider subsonic flow. (See fig. 2(a).) Two possible resulting variations of $\bar{L}$ are shown in the following

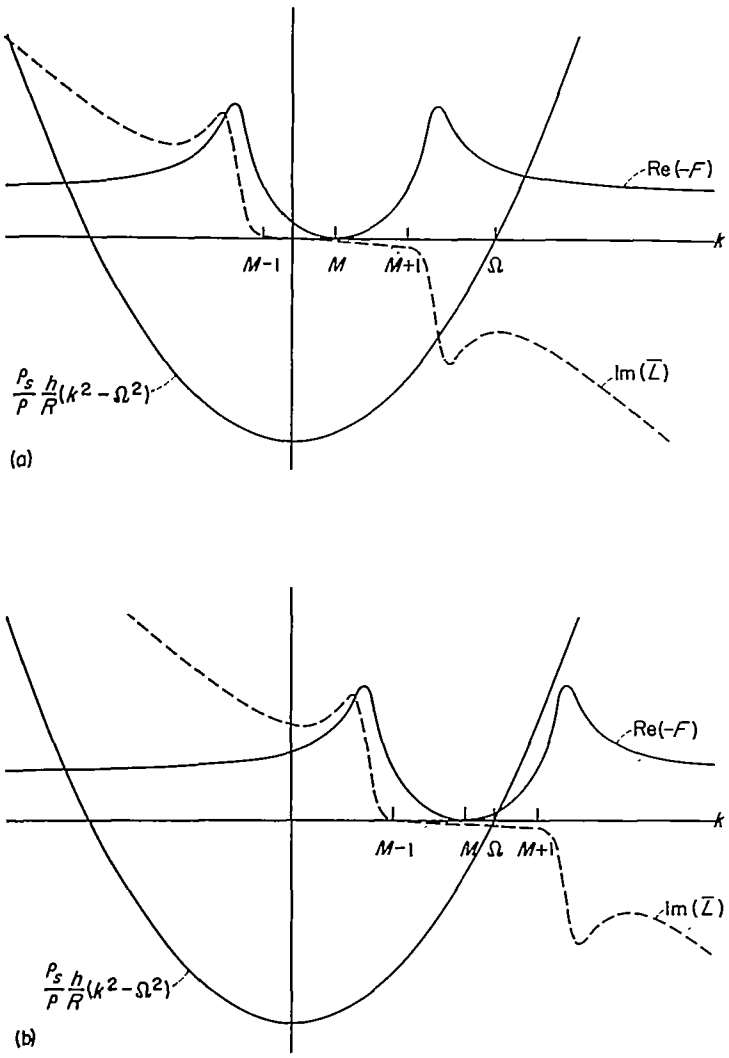

(a) Subsonic flow ($M<1$).
(b) Supersonic flow ($M>1$).

FIGURE 2.—Typical variations with k of functions comprising $\overline{L}$. (See eq. (9).)

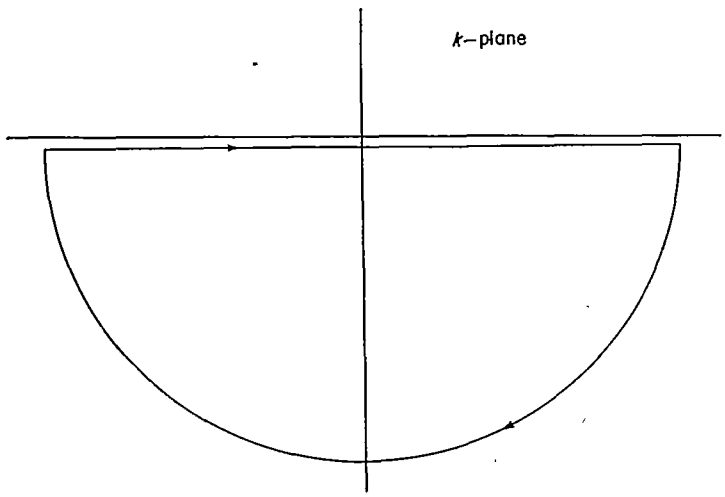

FIGURE 3.—Path enclosing lower half of k-plane (corresponding to unstable motion for $\bar{\nu}>0$).

Nyquist diagram (where the full circle at infinity corresponds to the infinite semicircle in the k-plane):

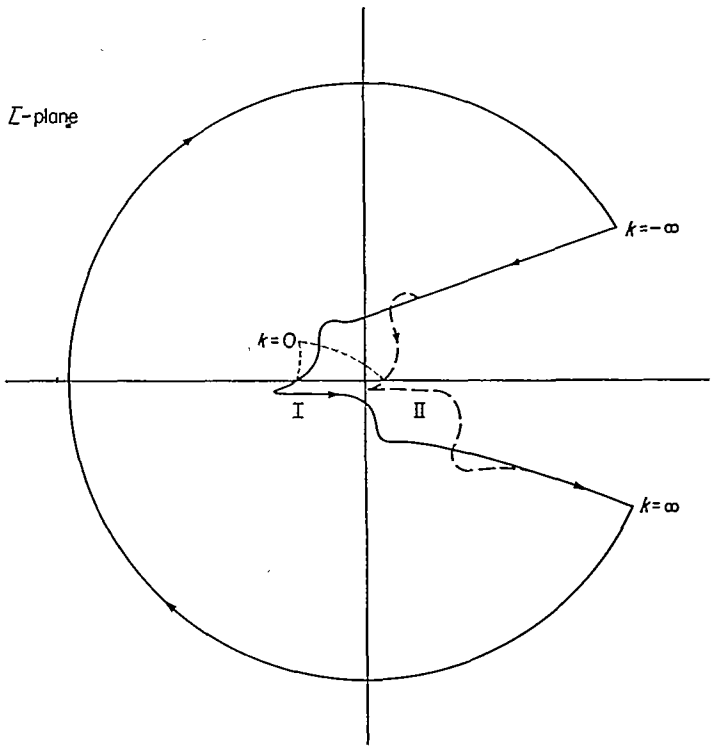

Sketch 1.

For different values of the parameters, paths similar to I or II may be traced. For path I, there is no encirclement of the origin and the cylinder is stable; for path II, on the other hand, one encirclement occurs and the cylinder is unstable. Since, by virtue of the damping term, $\mathrm{Im}(\overline{L})$ must pass through zero at $k=0$, it is apparent that the boundary between these two conditions is a static (divergence) boundary defined throughout the subsonic range by

$$\mathrm{Re}\,(\overline{L})_{k=0}=0=-\frac{\rho_s}{\rho}\frac{h}{R}\,\Omega^2-F(M,\bar{\nu},n) \tag{10}$$

Equation (10) may be put into the form

$$\left(\frac{h}{R}\right)^3+A\,\frac{h}{R}-B=0 \tag{11}$$

where

$$A=\frac{12(1-\mu^2)}{\bar{\nu}^2\left(1+\frac{n^2}{\bar{\nu}^2}\right)^2}\left[\frac{1}{\bar{\nu}^2\left(1+\frac{n^2}{\bar{\nu}^2}\right)^2}+\bar{\sigma}_x+\frac{n^2}{\bar{\nu}^2}\,\bar{\sigma}_\theta\right]$$

and

$$B=-\frac{12(1-\mu^2)}{\frac{\rho_s}{\rho}\left(\frac{c_s}{c}\right)^2}\,\frac{F(M,\bar{\nu},n)}{\bar{\nu}^2\left(1+\frac{n^2}{\bar{\nu}^2}\right)^2}$$

are positive numbers. Equation (11) has the one real root

$$\frac{h}{R}=\left(\frac{B}{2}+\sqrt{\frac{B^2}{4}+\frac{A^3}{27}}\right)^{1/3}+\left(\frac{B}{2}-\sqrt{\frac{B^2}{4}+\frac{A^3}{27}}\right)^{1/3} \tag{12}$$

Thus, for selected values of the other parameters, the thickness ratio corresponding to the stability boundary in

the subsonic range may be computed directly. This is the bounding value of h/R above which the cylinder is stable. For certain ranges of the parameters, namely when the Mach number is only slightly less than 1 or when the wave length of flutter is very large, the approximation $F(M,\bar{\nu},n)\approx-\frac{M^2}{n}$ is permissible. When this approximation is valid, equation (10) may be solved directly for M to yield

$$M\approx\sqrt{n\frac{\rho_s}{\rho}\frac{h}{R}\Omega^2}\qquad\left(\frac{\bar{\nu}^2(1-M^2)}{2n(n-1)}\ll 1\right)\tag{13}$$

Equation (13) gives the approximate bounding value of M below which the cylinder is stable.

For supersonic flow (fig. 2(b)), the possible Nyquist diagrams resulting when k traverses the path of figure 3 appear as shown in sketch 2.

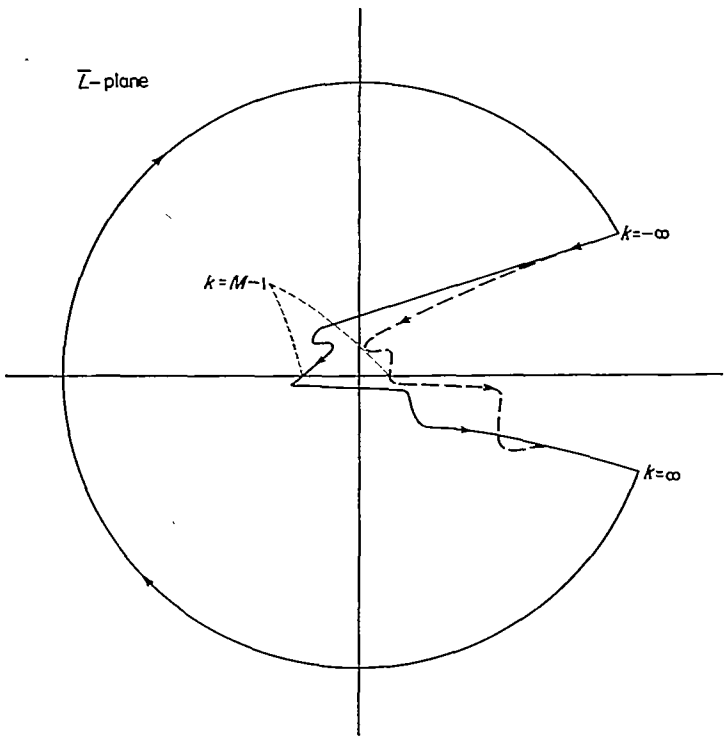

Sketch 2.

Since, now, the sign of the imaginary part of $\bar{L}$ always changes at $k=M-1$, the criterion for a boundary is seen to be

$$\mathrm{Re}\,(\bar{L})_{k=M-1}=0=\frac{\rho_s}{\rho}\frac{h}{R}\left[(M-1)^2-\Omega^2\right]-F(1,\bar{\nu},n)\tag{14}$$

Thus, the instability is dynamic, and, since $k=\frac{\omega}{\nu c}$, the flutter mode is a traveling wave whose propagation velocity $\frac{\omega}{\nu}$ is the velocity of external flow minus the velocity of sound.

The solution of equation (14) for h/R can be carried out to yield a result in the same form as equation (12) with appropriate redefinition of A and B. In the supersonic case, however, the F-function is independent of M and is actually equal to $-1/n$; hence, equation (14) may be solved directly for the Mach number of flutter to give the convenient form

$$M=1+\sqrt{\Omega^2-\frac{1}{n\frac{\rho_s}{\rho}\frac{h}{R}}}\tag{15}$$

Determination of critical stability boundary.—In computing stability boundaries, a factor which must be kept in mind is the admissibility of all longitudinal wave lengths and of all integral values of n greater than or equal to 2. The critical boundary must necessarily correspond to the values of $\bar{\nu}$ and n for which the cylinder is most prone to flutter. This critical boundary can be obtained either by expressing the bounding value of h/R as a function of the rest of the parameters (as in eq. (12)) and maximizing this value of h/R with respect to both $\bar{\nu}$ and n or by finding the bounding value of M (as in eqs. (13) and (15)) and minimizing with respect to $\bar{\nu}$ and n. Of the two alternatives, the latter is more easily accomplished, analytical minimization of M being possible. For subsonic speeds, however, the expression for M (eq. (13)) is only approximate and, in some instances, it becomes necessary to maximize h/R as given by equation (12). This is most readily achieved by graphical methods.

Minimization of M can be performed by first minimizing Ω^2 with respect to $\bar{\nu}$ and then minimizing the resulting M with respect to n. The minimization with respect to $\bar{\nu}$ is particularly simple when there are no imposed midplane stresses ($\sigma_x=\sigma_\theta=0$); it can be performed with respect to the quantity $\left(\bar{\nu}+\frac{n^2}{\bar{\nu}}\right)^2$. The result is

$$\Omega_{min}^2=\frac{2\left(\frac{c_s}{c}\right)^2\frac{h}{R}}{\sqrt{12(1-\mu)^2}}\tag{16}$$

at

$$\left(\bar{\nu}+\frac{n^2}{\bar{\nu}}\right)^2=\frac{\sqrt{12(1-\mu^2)}}{\frac{h}{R}}\tag{17}$$

However, the quantity $\left(\bar{\nu}+\frac{n^2}{\bar{\nu}}\right)^2$ is itself a minimum at $\bar{\nu}=n$; hence, equation (17) can be satisfied only when

$$\frac{\sqrt{12(1-\mu^2)}}{\frac{h}{R}}>4n^2\tag{18}$$

and, if this condition is violated, Ω^2 can never achieve the value given by equation (16). The minimum value it can achieve is

$$\Omega_{min}^2=\left(\frac{c_s}{c}\right)^2\left[\frac{4\left(\frac{h}{R}\right)^2n^2}{12(1-\mu^2)}+\frac{1}{4n^2}\right]\tag{19}$$

If the result given by either equation (16) or equation (19) is substituted into equation (15), the minimum value of M is seen to correspond to the smallest admissible value of n

(that is, $n=2$); hence, for supersonic flow, the critical boundary is given by

$$\left.\begin{aligned} M_{cr}&=1+\sqrt{\frac{2\left(\frac{c_s}{c}\right)^2\frac{h}{R}}{\sqrt{12(1-\mu^2)}}-\frac{1}{2\frac{\rho_s}{\rho}\frac{h}{R}}} && \left(\frac{h}{R}<\frac{\sqrt{12(1-\mu^2)}}{16}\right)\\ &=1+\sqrt{\left(\frac{c_s}{c}\right)^2\left[\frac{16\left(\frac{h}{R}\right)^2}{12(1-\mu^2)}+\frac{1}{16}\right]-\frac{1}{2\frac{\rho_s}{\rho}\frac{h}{R}}} && \left(\frac{h}{R}>\frac{\sqrt{12(1-\mu^2)}}{16}\right)\end{aligned}\right\} \tag{20}$$

Similarly, for subsonic flow, if the approximate equation, equation (13), is valid, the substitution of equation (16) into equation (13) yields the critical boundary

$$M_{cr}\approx\sqrt{4\frac{\rho_s}{\rho}\left(\frac{c_s}{c}\right)^2\frac{\left(\frac{h}{R}\right)^2}{\sqrt{12(1-\mu^2)}}}\quad\left((1-M_{cr}^2)\frac{4\frac{h}{R}}{\sqrt{12(1-\mu^2)}}\ll 1\right) \tag{21}$$

Numerical example.—For illustrative purposes, the critical stability boundary ($n=2$) has been computed for an empty, unstressed aluminum cylinder at sea level; additional curves corresponding to $n=3$, 4, 5, and 10 have been obtained for comparison. These results are shown by the solid curves in figure 4. Portions of the curves in the subsonic range were obtained by graphically maximizing h/R with respect to $\bar{\nu}$ as previously mentioned. It is interesting to examine the wave lengths of the flutter modes corresponding to these boundaries. In the range where equation (18) is satisfied, solution of equation (17) yields two different wave lengths for the same critical thickness ratio. The larger one of these two wave lengths is shown in figure 5 for supersonic Mach numbers in the form of a plot of the aspect ratio of the flutter mode $n/\bar{\nu}$ (the ratio of longitudinal to circumferential wave length) against Mach number for $n=2$, 3, 4, and 5. The aspect ratios associated with the smaller wave lengths are not plotted; they are merely the reciprocals of the ones shown. At the higher Mach numbers, the critical value of h/R becomes large enough to cause equation (18) to be violated; when this happens, the two flutter modes coalesce to give a single flutter aspect ratio of unity as shown by the horizontal cutoff line in figure 5.

As has been pointed out, Donnell's theory is somewhat inaccurate for small values of n. (See, for example, ref. 12.) In order to obtain some idea of the magnitude of the resulting error, a new Ω-function based on a simplified version of Flügge's cylindrical-shell theory (see, for example, refs. 11 and 12) has been derived and minimized with respect to $\bar{\nu}$;

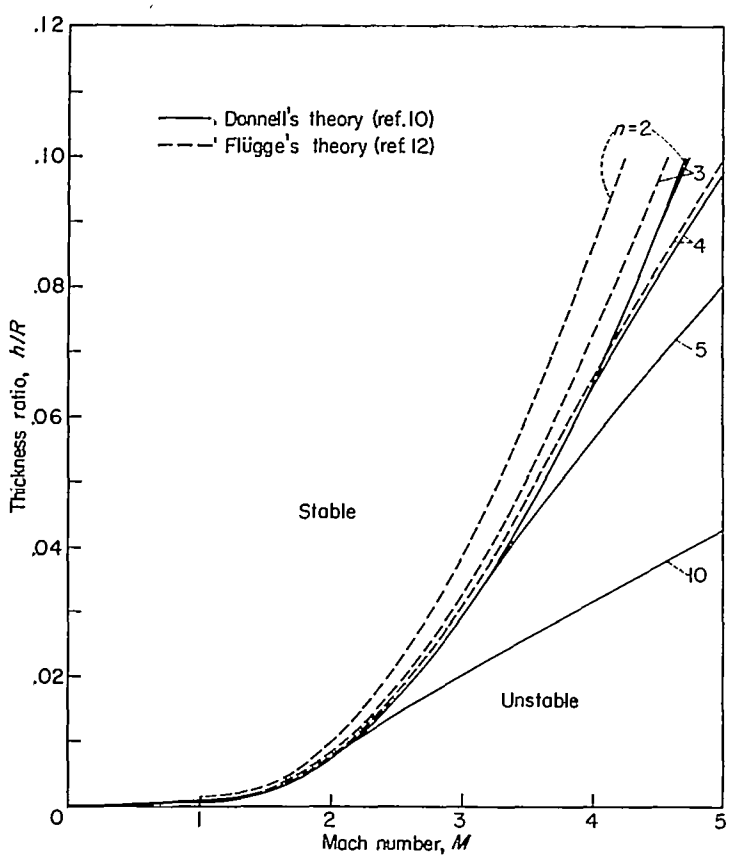

FIGURE 4.—Stability boundaries for empty, infinitely long, unstiffened aluminum cylinder at sea level with no applied membrane stress.

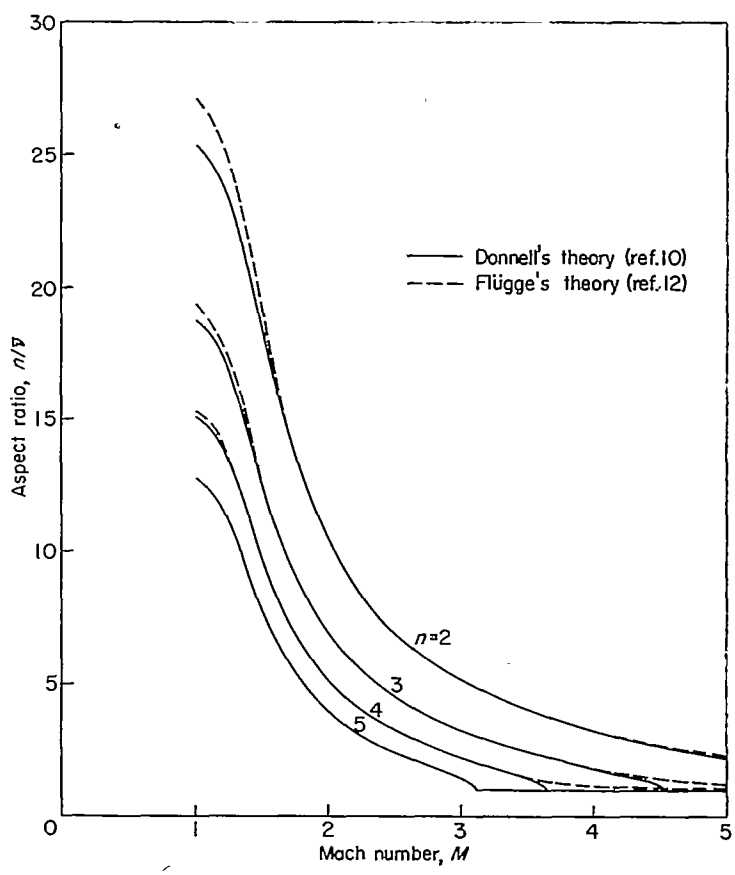

FIGURE 5.—Panel aspect ratio of critical flutter mode for empty, infinitely long, unstiffened aluminum cylinder at sea level with no applied membrane stress.

the details of this derivation are presented in appendix C. Computations in the supersonic range with the new (Flügge) Ω-function result in the dashed curves shown in figures 4 and 5. As in Donnell's theory, the Flügge theory yields, for the lower thickness ratios, two values of wave length for which Ω (and, hence, the Mach number) is a minimum. In contrast with Donnell's theory, however, the two wave lengths are not equally critical; the larger one always yields a lower Mach number. For this reason, only the higher aspect ratio and its associated stability boundary are plotted in the figures. The critical boundary ($n=2$) is found to require thickness ratios approximately 30 percent higher than those predicted by Donnell's theory. The two curves for $n=3$ still differ by 10 to 15 percent; but, for $n=4$, the two theories agree very well. For the sake of clarity, the stability boundary associated with the lower aspect ratio has not been shown in figure 4. It should be remarked, however, that this boundary agrees very well with the boundary given by Donnell's theory, even for $n=2$. The practical implications of the results shown in figures 4 and 5 are discussed subsequently.

ANALYSIS OF FLUID-FILLED CYLINDER

When the cylinder is assumed to contain a fluid, the additional term $\frac{\rho_f}{\rho}\left(\frac{c_f}{c}\right)^2 F_f\left(\frac{c}{c_f}k,\bar{\nu},n\right)$ in equation (8) must be included. A typical plot of this function for real values of k is shown in figure 6. Note that the force is always real and becomes infinite at the resonant frequencies

$$k_j=\frac{c_f}{c}\sqrt{1+\frac{z_j^2}{\bar{\nu}^2}} \qquad (j=1,2,3,\ldots) \tag{22}$$

where the z_j's are the zeros of $J_n'(z)$.

Since F_f is always real for real values of k, the imaginary part of L can again be zero only at $k=0$ in the subsonic range and at $k=M-1$ in the supersonic range. Stability boundaries can consequently occur only at these frequencies. In the subsonic range, the inclusion of F_f has no effect upon the stability boundaries since $F_f=0$ at $k=0$. In the supersonic range, however, the inclusion of F_f has a considerable effect on the stability boundaries, not only because of the additional force at $k=M-1$ but also because of the resonances of F_f.

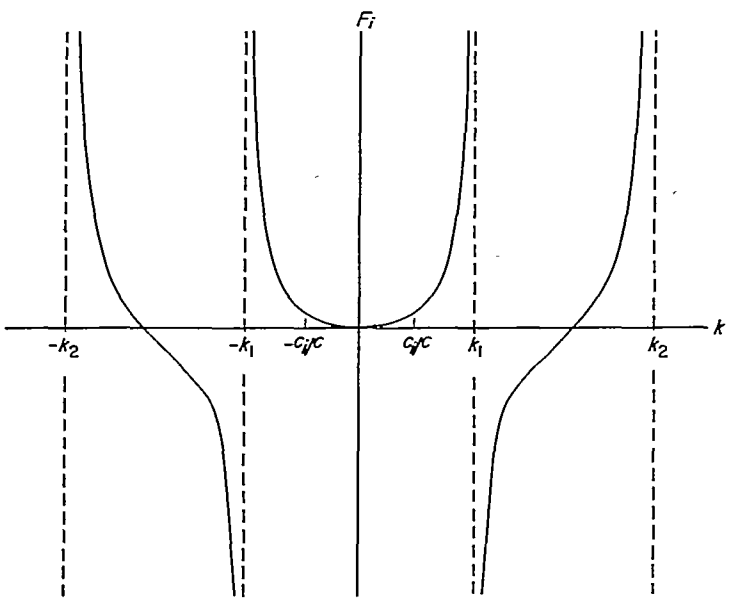

FIGURE 6.—Typical variation of F_f with k.

The condition for the stability boundary at supersonic speeds is

$$\mathrm{Re}(L)_{k=M-1}=0=\frac{\rho_s}{\rho}\frac{h}{R}\left[(M-1)^2-\Omega^2\right]+\frac{1}{n}+\frac{\rho_f}{\rho}\left(\frac{c_f}{c}\right)^2 F_f\left[\frac{c}{c_f}(M-1),\bar{\nu},n\right] \tag{23}$$

This equation can be solved for h/R in the same form as equation (12); that is,

$$\frac{h}{R}=\left(\frac{B}{2}+\sqrt{\frac{B^2}{4}+\frac{A^3}{27}}\right)^{1/3}+\left(\frac{B}{2}-\sqrt{\frac{B^2}{4}+\frac{A^3}{27}}\right)^{1/3} \tag{24}$$

where now

$$A=\frac{12(1-\mu^2)}{\bar{\nu}^2\left(1+\frac{n^2}{\bar{\nu}^2}\right)^2}\left[\frac{1}{\bar{\nu}^2\left(1+\frac{n^2}{\bar{\nu}^2}\right)^2}+\bar{\sigma}_x+\frac{n^2}{\bar{\nu}^2}\bar{\sigma}_\theta-\frac{(M-1)^2}{\left(\frac{c_s}{c}\right)^2}\right]$$

and

$$B=\frac{12(1-\mu^2)}{\bar{\nu}^2\left(1+\frac{n^2}{\bar{\nu}^2}\right)^2}\frac{1}{\frac{\rho_s}{\rho}\left(\frac{c_s}{c}\right)^2}\left[\frac{1}{n}+\frac{\rho_f}{\rho}\left(\frac{c_f}{c}\right)^2 F_f\left(\frac{c}{c_f}(M-1),\bar{\nu},n\right)\right]$$

The variation of h/R with Mach number for particular values of the other parameters is shown in sketch 3. Note

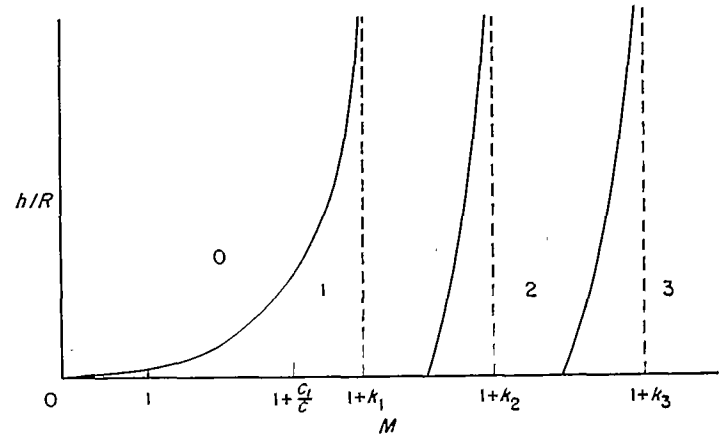

Sketch 3.

that h/R becomes infinite when the Mach number is equal to $1+k_j$ ($j=1, 2, 3, \ldots$). (See eq. (22).) This arises from the infiniteness of F_f and, consequently, of B at these Mach numbers. Note also that the footpoints of the secondary stability boundaries occur when $B=0$. The numbers within the regions separated by the solid lines indicate the degree of instability as determined by use of Nyquist diagrams.

Since the value of h/R for the empty cylinder is given by equation (24) with F_i equal to zero, and since F_i is positive for values of M less than $1+k_1$, it can be seen that the fluid inside the cylinder has a destabilizing effect.

In order to find the critical stability boundaries, all values of $\bar{\nu}$ and n must be considered. Of particular interest in this connection is the fact that, for very large values of $\bar{\nu}$, the infinities shown in the sketch all approach a value of M equal to $1+\frac{c_i}{c}$. (See eq. (22).) Thus, the critical stability boundaries would appear as shown in sketch 4. For Mach numbers

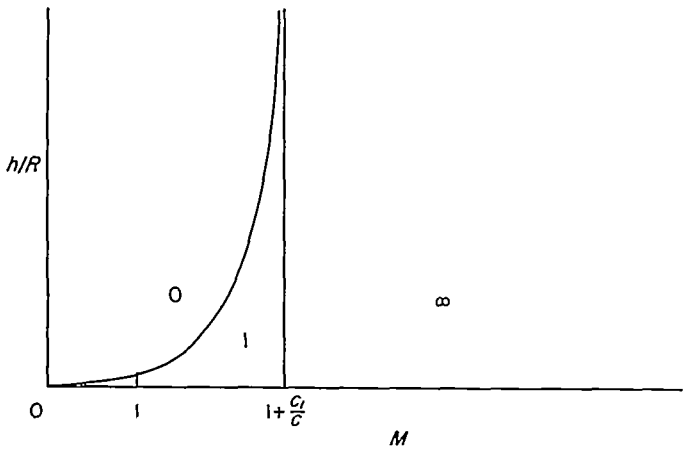

Sketch 4.

greater than $1+\frac{c_i}{c}$, the cylinder is unstable to an infinite degree. If the fluid inside the cylinder is air at the same temperature as the surrounding air, this limiting Mach number would be equal to 2. If the cylinder contains a relatively incompressible fluid, however, this Mach number could be very high. In any event, the result is somewhat anomalous; it is probably caused by the use of linearized potential-flow theory and, undoubtedly, would not occur for real fluids.

SOME REMARKS ABOUT THE SOLUTION FOR AN UNSTIFFENED CYLINDER

On damping.—The stability criteria for the infinitely long, unstiffened cylinder which were derived in the preceding sections were obtained by including the effects of structural damping and then taking the limit as the damping approached zero ($\epsilon \rightarrow 0$). This procedure was followed because different criteria are obtained when damping is not considered ($\epsilon \equiv 0$). This important fact is illustrated in appendix D where the stability criteria for the empty cylinder with zero damping are discussed. Since structures always exhibit some damping, it is apparent that stability criteria obtained by taking the limit as ϵ approaches zero are more realistic than those obtained by setting ϵ identically equal to zero. It is interesting to note that, in this case, the addition of damping makes the structure more prone to flutter. This somewhat surprising result may be explained by the fact that a damping force, even though in itself dissipative, can cause phase changes in such a manner as to allow the moving outside air to feed more energy into the structure; the result is a net energy gain.

On the effects of midplane stresses.—The qualitative effects on flutter of the midplane tension stresses σ_x and σ_θ (arising, say, from a static-pressure differential across the cylinder wall) may be determined by considering the definition of the wave speed Ω yielded by the Donnell theory (immediately following eq. (8)). As expected, both σ_x and σ_θ contribute to increased stability since they increase Ω and, hence, Mach number (see eq. (15)). Perhaps most significant, however, is the influence of midplane stress on the predicted wave length of the flutter mode. Note that, while the presence of σ_x stresses increases Ω uniformly for all wave lengths, the increase due to σ_θ is proportional to the square of the aspect ratio $n/\bar{\nu}$. Thus, the two minima of Ω are no longer equally critical; the smaller minimum (and, hence, the most critical boundary) is seen to correspond to the shorter longitudinal waves. This is opposite to the result yielded by the more accurate Flügge theory for the cylinder without midplane stress; thus, it would appear that addition of enough circumferential stress to the Flügge theory might produce a shift of the critical flutter mode from one with very long waves to one with very short waves. This possibility is important since results for an infinitely long cylinder would be applicable to a finite cylinder only if the wave lengths of the flutter modes were small in comparison with the length of the finite structure.

Thus, in spite of the results yielded by the analyses of the unstressed cylinder pertaining to the wave length of flutter, it must not be concluded that analysis of an infinitely long cylinder has no application to cylinders of finite length. In fact, it may well be that, even for the unstressed cylinder, the minimum Ω corresponding to the predicted most critical flutter mode (with long waves) should be arbitrarily ignored in favor of the secondary minimum. Then, in view of the aforementioned agreement between Flügge's and Donnell's theories at this minimum, the Donnell theory would be adequate for all $n(\geqq 2)$, the critical boundary being specified by the solid curve for $n=2$ in figure 4. The aspect ratio of the flutter mode, in this case, would be the reciprocal of the value given in figure 5.

On the effect of longitudinal stringers.—Although the analysis has been carried out for the case of an unstiffened cylinder, the flutter criteria may also be applied to the case of a cylinder with essentially rigid, longitudinal stiffeners. These longitudinal stiffeners would have the effect of raising the minimum value of n and, hence, of decreasing the critical thickness ratio of flutter. For example, the curve for 20 stringers ($n=10$) has been plotted in figure 4.

This completes the discussion of unstiffened cylinders; an analysis of ring-stiffened cylinders is presented in the next section.

RING-STIFFENED CYLINDER

The ring-stiffened cylinder consists of the unstiffened cylinder with added, rigid ring stiffeners which prevent radial deflection at the locations $x=\pm ja$ ($j=0, 1, 2, \ldots$). (See fig. 1(b).) The stiffeners are assumed not to interfere with the flow of air outside or of fluid inside the cylinder. The analysis proceeds along the lines of that in reference 7.

DERIVATION OF EQUATIONS

If the assumptions are made that the cylinder wall may deform into any number of sinusoidal waves around its circumference and into any shape periodic over 2 bay lengths in the longitudinal direction, the deformation may be written, with complete generality, as

$$w(x,\theta,t)=\mathrm{Re}\left(\sum_{m=-\infty}^{\infty} a_m e^{-i\frac{m\pi x}{a}} e^{i\omega t}\cos n\theta\right) \tag{25}$$

provided that the coefficients a_m satisfy the constraining relations

$$\left.\begin{aligned}\sum_{m=-\infty}^{\infty} a_m&=0\\ \sum_{m=-\infty}^{\infty}(-1)^m a_m&=0\end{aligned}\right\} \tag{26}$$

These conditions correspond to zero deflection at the ring locations. They may also be written as

$$\left.\begin{aligned}\sum_{\substack{m=-\infty\\(m\ odd)}}^{\infty} a_m&=0\\ \sum_{\substack{m=-\infty\\(m\ even)}}^{\infty} a_m&=0\end{aligned}\right\} \tag{27}$$

Only one circumferential term is included in equation (25) because there is no structural or aerodynamic coupling between the various cosine terms. Also, in this case, $n=1$ is admitted. The assumption of periodicity over 2 bay lengths is made because it permits a considerable degree of generality without overcomplicating the analysis. It is believed that the critical flutter mode would be of this type.

Air forces.—In view of the linearity of the aerodynamic theory, the air forces exerted on a cylinder executing the motion given by equation (25) may be determined by separately considering each term of the summation over m and superposing the results. Hence, the aerodynamic loading on a cylinder deforming in the shape of the traveling wave

$$w_m(x,\theta,t)=\mathrm{Re}\left[a_m e^{-i\frac{m\pi}{a}\left(x-\frac{\omega a}{m\pi}t\right)}\cos n\theta\right] \tag{28}$$

is sought.

If equation (28) is compared with equation (1), it becomes apparent that the air force is given by equations (3) to (6) when the substitutions $\overline{w}=a_m$ and $\nu=m\pi/a$ are made. Thus, the total air force may be written immediately as

$$l(x,\theta,t)=R\frac{\pi^2}{a^2}\mathrm{Re}\left(\sum_{m=-\infty}^{\infty} l_m a_m e^{-i\frac{m\pi x}{a}} e^{i\omega t}\cos n\theta\right) \tag{29}$$

where, for $m\neq 0$,

$$l_m=-\rho c^2 m^2 F\left(M-\frac{k}{m},\ m\alpha,n\right)+\rho_i c_i^2 m^2 F_i\left(\frac{c}{c_i}\frac{k}{m},\ m\alpha,n\right) \tag{30}$$

The functions F and F_i are given by equations (5) and (6). They are repeated here for convenience.

$$\left.\begin{aligned}F(\xi,b,n)&=\xi^2\frac{K_n(\zeta)}{\zeta K_n'(\zeta)} && (|\xi|<1)\\ &=\xi^2\frac{H_n^{(j)}(z)}{zH_n^{(j)\prime}(z)}\quad\left(j=\begin{cases}1\text{ for }b\xi>0\\2\text{ for }b\xi<0\end{cases}\right) && (|\xi|>1)\end{aligned}\right\} \tag{31}$$

$$\left.\begin{aligned}F_i(\xi,b,n)&=\xi^2\frac{I_n(\zeta)}{\zeta I_n'(\zeta)} && (|\xi|<1)\\ &=\xi^2\frac{J_n(z)}{zJ_n'(z)} && (|\xi|>1)\end{aligned}\right\} \tag{32}$$

where

$$\zeta=|b|\sqrt{1-\xi^2}$$

$$z=|b|\sqrt{\xi^2-1}$$

In equation (30), $k=\omega a/\pi c$ and $\alpha=R\pi/a$. The quantity α is the ratio of one-half the circumference to the distance between the rings. For the special case of $m=0$, a limiting process gives

$$l_0=-\rho c^2 G(k,\alpha,n)+\rho_i c_i^2 G_i\left(\frac{c}{c_i}k,\alpha,n\right) \tag{33}$$

In equation (33),

$$G(\xi,\alpha,n)=\xi^2\frac{H_n^{(j)}(\alpha|\xi|)}{\alpha|\xi|H_n^{(j)\prime}(\alpha|\xi|)}\quad\left(j=\begin{cases}1\text{ for }\xi<0\\2\text{ for }\xi>0\end{cases}\right) \tag{34}$$

$$G_i(\xi,\alpha,n)=\xi^2\frac{J_n(\alpha|\xi|)}{\alpha|\xi|J_n'(\alpha|\xi|)} \tag{35}$$

Equilibrium conditions.—By virtue of the assumed longitudinal spatial periodicity of the deformation, satisfaction of equilibrium over any interval of length $2a$ assures satisfaction of equilibrium over the whole length of the cylinder. Thus, it is sufficient to write Donnell's equation for the segment $0\leq x<2a$ as

$$D\left[\nabla^4 w+\frac{1}{R^4}\frac{12(1-\mu^2)}{\left(\frac{h}{R}\right)^2}\nabla^{-4}w_{xxxx}\right]-h\left(\sigma_x w_{xx}+\frac{\sigma_\theta}{R^2}w_{\theta\theta}\right)+$$

$$\rho_s h w_{tt}=l(x,\theta,t)+P_0(\theta,t)\delta(x)+P_1(\theta,t)\delta(x-a) \tag{36}$$

where P_0 and P_1 are the reaction forces exerted on the cylinder wall by the two ring stiffeners included in the interval and where $\delta(x)$ is the Dirac delta function.

Let

$$\left.\begin{aligned}P_0(\theta,t)&=\mathrm{Re}(\overline{P}_0 e^{i\omega t}\cos n\theta)\\ P_1(\theta,t)&=\mathrm{Re}(\overline{P}_1 e^{i\omega t}\cos n\theta)\end{aligned}\right\} \tag{37}$$

If P_0 and P_1 from equations (37), w from equation (25), and l from equation (29) are substituted into the equilibrium equation, equation (36), and if this equation is then multiplied by $e^{\frac{im\pi x}{a}}$ and integrated over the interval, there

results

$$2a\left\{D\left[\left(\frac{m^2\pi^2}{a^2}+\frac{n^2}{R^2}\right)^2+\frac{12(1-\mu^2)}{R^4\left(\frac{h}{R}\right)^2}\frac{\left(\frac{m\pi}{a}\right)^4}{\left(\frac{m^2\pi^2}{a^2}+\frac{n^2}{R^2}\right)^2}\right]+h\left(\frac{m^2\pi^2}{a^2}\sigma_x+\frac{n^2}{R^2}\sigma_\theta\right)-\rho_s h\omega^2-R\frac{\pi^2}{a^2}l_m\right\}a_m=\overline{P}_0+(-1)^m\overline{P}_1$$

$$(m=0,\pm1,\pm2,\pm3,\ldots) \quad (38)$$

Hence, for $\beta_m\neq0$,

$$a_m=\frac{\overline{P}_0+(-1)^m\overline{P}_1}{\frac{2\pi^2c^2\rho R}{a}\beta_m} \quad (39)$$

where, for $m\neq0$,

$$\beta_m=\frac{\rho_s}{\rho}\frac{h}{R}(\Omega_m^2-k^2)-\frac{\rho_t}{\rho}\left(\frac{c_t}{c}\right)^2m^2F_t\left(\frac{c}{c_t}\frac{k}{m},m\alpha,n\right)+m^2F\left(M-\frac{k}{m},m\alpha,n\right)+i\frac{m}{|m|}\epsilon_m k$$

with

$$\Omega_m=\frac{\frac{c_s}{c}\frac{h}{R}m}{\sqrt{12(1-\mu^2)}}\sqrt{n^2\left(\frac{m\alpha}{n}+\frac{n}{m\alpha}\right)^2+\frac{12(1-\mu^2)}{\left(\frac{h}{R}\right)^2}\left[\frac{1}{n^2\left(\frac{m\alpha}{n}+\frac{n}{m\alpha}\right)^2}+\overline{\sigma}_x+\left(\frac{n}{m\alpha}\right)^2\overline{\sigma}_\theta\right]}$$

Note that, as in the case of the unstiffened cylinder, a term has been added to each of the β_m's to approximate the effect of damping ($\epsilon_m>0$). In the limit as $m\to0$,

$$\beta_0=\frac{\rho_s}{\rho}\frac{h}{R}(\Omega_0^2-k^2)-\frac{\rho_t}{\rho}\left(\frac{c_t}{c}\right)^2G_t\left(\frac{c}{c_t}k,\alpha,n\right)+G(k,\alpha,n)+i\epsilon_0k$$

where

$$\Omega_0=\frac{\frac{c_s}{c}\frac{h}{R}}{\sqrt{12(1-\mu^2)}}\frac{n}{\alpha}\sqrt{n^2+\frac{12(1-\mu^2)}{\left(\frac{h}{R}\right)^2}\overline{\sigma}_\theta}$$

Finally, substituting from equation (39) into the constraining relations, equations (27), gives the following conditions for the existence of the motion defined by equation (25):

$$(\overline{P}_0-\overline{P}_1)\sum_{\substack{m=-\infty\\(m\ odd)}}^{\infty}\frac{1}{\beta_m}=0 \quad (40)$$

$$(\overline{P}_0+\overline{P}_1)\sum_{\substack{m=-\infty\\(m\ even)}}^{\infty}\frac{1}{\beta_m}=0 \quad (41)$$

Inspection of these relations indicates that simultaneous satisfaction of the equilibrium equation and the restraint conditions can be achieved in a nontrivial fashion in several independent ways. One possibility is that

$$\overline{P}_0=\overline{P}_1$$

(which implies that $a_m=0$ when m is odd) and

$$\sum_{\substack{m=-\infty\\(m\ even)}}^{\infty}\frac{1}{\beta_m}=0 \quad (42)$$

and another is that

$$\overline{P}_0=-\overline{P}_1$$

(which implies that $a_m=0$ when m is even) and

$$\sum_{\substack{m=-\infty\\(m\ odd)}}^{\infty}\frac{1}{\beta_m}=0 \quad (43)$$

As has been noted, the derivation herein and the results achieved exactly parallel those obtained in reference 7 for the infinite, flat plate. As pointed out therein, still another nontrivial solution is found when the restriction $\beta_m\neq0$ (which characterized the foregoing results) is removed. Specifically, if two or more β_m's of the same type (m odd or even) vanish simultaneously, a flutter mode may exist.

Equations (42) and (43) are conditions for the existence of motion of constant amplitude; equation (42) corresponds to motion which is identical in each bay, whereas equation (43) corresponds to motion having the same amplitude from bay to bay but with alternating direction.

STABILITY BOUNDARIES

As in the case of the unstiffened cylinder, the Nyquist criterion can be used to investigate the states of stability of the stiffened cylinder. In this section are given the results of a limited investigation which was chiefly concerned with the examination of the following three-term approximation to equation (42):

$$N\equiv\frac{1}{\beta_0}+\frac{1}{\beta_2}+\frac{1}{\beta_{-2}}=0 \quad (44)$$

Subsonic flow.—In applying the Nyquist diagram technique to the function N, account must be taken of the poles of N at the zeros of β_2 and β_{-2}. (There are no zeros of β_0.) The results of such an application with $\epsilon\to0$ show clearly that, for subsonic Mach numbers, the only possible instability is divergence; further, the three-term approximation leads to as many as three static stability boundaries as shown in

sketch 5. In this sketch, a typical variation of $(h/R)_{max}$

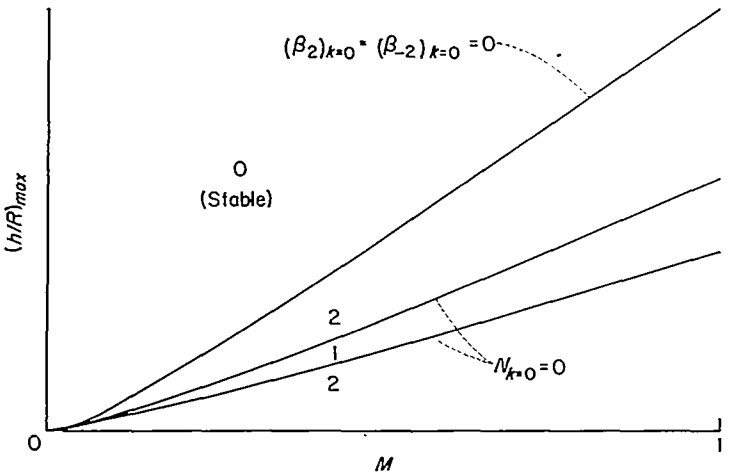

Sketch 5.

with M (with other pertinent parameters fixed) is shown. The subscript $_{max}$ indicates that the thickness ratio is maximized with respect to n. The numbers indicate the number of unstable roots of equation (44) corresponding to each region. Note that the upper curve corresponds to the condition that two or more β_m's of the same type vanish simultaneously, whereas the other curves result from the condition $(N)_{k=0}=0$.

Additional curves would result from the addition of more terms to N and still more curves would result from the consideration of the odd solution, equation (43); further, examination of a four-term approximation ($m=1$, -1, 3, and -3) to equation (43) indicates that, for reasonable values of α, the most critical boundary for either the even or the odd solution must stem from the condition $(\beta_1)_{k=0}=(\beta_{-1})_{k=0}=0$. (For very small values of α, the distance between rings becomes large and values of m other than unity may be critical.) The position of this critical boundary has been computed for an unstressed aluminum cylinder at sea level for various representative values of the aspect-ratio parameter α. The results are shown in figure 7. These curves correspond to various values of n ranging from 5 upward as illustrated on the plot; since n is large, Donnell's theory is sufficiently accurate.

Note that the thickness ratios required for static stability at subsonic Mach numbers are extremely small; therefore, divergence at subsonic speeds is probably not a critical design factor.

Supersonic flow.—Application of the Nyquist criteria for supersonic flow is not so readily accomplished without the performance of further computations. It is clear, however, that divergence boundaries extend into the supersonic range and that flutter boundaries arise which probably become more critical than the divergence boundaries.

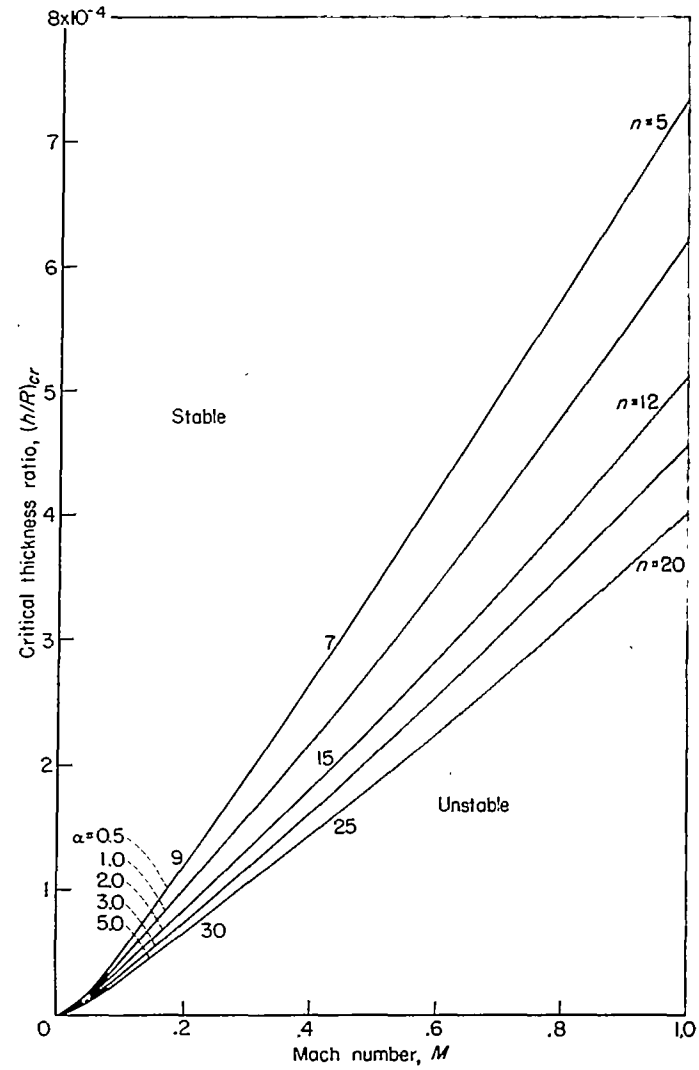

FIGURE 7.—Critical divergence boundaries for infinitely long, unstressed, ring-stiffened aluminum cylinder at sea level.

The definition of these flutter boundaries requires that solutions be obtained to equations (42) and (43) or to suitable approximations, such as equation (44). This, in turn, requires extensive computations, especially since the resulting thickness ratios must be maximized with respect to n. This maximization can probably only be achieved laboriously by making each computation for several values of n.

CONCLUDING REMARKS

A preliminary theoretical investigation of the aeroelastic stability of infinitely long, thin-walled unstiffened and ring-stiffened circular cylinders has been conducted by using Donnell's cylinder theory and linearized unsteady potential-flow theory. A limited study of the resulting stability criteria has yielded the following information.

For unstiffened cylinders with vanishingly small structural

damping, the only possible instability at subsonic Mach numbers is static divergence; in supersonic flow, however, flutter is found to occur for sufficiently thin cylinders in the form of a traveling wave whose propagation velocity is the velocity of the external flow minus the speed of sound. For an empty, unstressed aluminum cylinder at sea level, the critical boundary is found to correspond to a mode of deformation having only two waves around the circumference but a very large longitudinal wave length. For this case, the use of the more complicated cylinder theory of Flügge is necessary for accurate determination of the critical ratios of cylinder-wall thickness to radius. These are found to be relatively large.

Consideration of the effects of midplane tension stresses not only shows them to be stabilizing but indicates that large circumferential stress shifts the critical flutter condition from the mode with very long longitudinal waves to one with very short longitudinal waves for which Donnell's theory is adequate. The magnitude of the stabilizing influence of the midplane stresses has not been investigated.

The addition of an internal fluid has a destabilizing effect on the unstiffened cylinder. In fact, the anomalous result is found that for Mach numbers greater than 1 plus the ratio of the speeds of sound in the fluids inside and outside the cylinder, no adjustment of the physical properties of the cylinder will render it stable.

The presence of even the smallest amount of structural damping is found to be an important factor in analyses of infinitely long, unstiffened cylinders.

For the ring-stiffened cylinder it is found that flutter is not possible at subsonic Mach numbers and that only very small thickness ratios are required to prevent divergence. Although both panel flutter and divergence are possible at supersonic Mach numbers, no numerical results have been obtained; extensive computations would be required for a complete determination of the stability boundaries in this range.

Langley Aeronautical Laboratory,
National Advisory Committee for Aeronautics,
Langley Field, Va., *January 11, 1956.*

APPENDIX A

STEADY LINEARIZED FLOW PAST A STATIONARY DEFORMED CYLINDER

In this appendix are derived the perturbation pressures exerted by a steady external or internal flow of Mach number M_1 on an infinitely long thin-walled cylinder with the deformation

$$w=\mathrm{Re}(\overline{w}e^{-i\nu x_1}\cos n\theta) \tag{A1}$$

where n is a positive integer and the wave number ν may be either positive or negative. The Mach number M_1 is positive for flow in the positive x_1-direction and negative for flow in the negative x_1-direction. (See fig. 8.)

In the cylindrical coordinate system (x_1, r, θ), the linearized potential-flow equation is

$$(1-M_1^2)\phi_{x_1x_1}+\phi_{rr}+\frac{1}{r}\phi_r+\frac{1}{r^2}\phi_{\theta\theta}=0 \tag{A2}$$

where ϕ is the velocity potential and the subscripts x_1, r, and θ indicate differentiation with respect to these parameters. With the assumption that

$$\phi(x_1,r,\theta)=\mathrm{Re}[f(r)e^{-i\nu x_1}\cos n\theta] \tag{A3}$$

equation (A2) becomes

$$f_{rr}+\frac{1}{r}f_r+\left[\nu^2(M_1^2-1)-\frac{n^2}{r^2}\right]f=0 \tag{A4}$$

which, for supersonic flow ($|M_1|>1$), has the solution

$$f(r)=AH_n^{(1)}(|\nu|\sqrt{M_1^2-1}r)+BH_n^{(2)}(|\nu|\sqrt{M_1^2-1}r) \tag{A5}$$

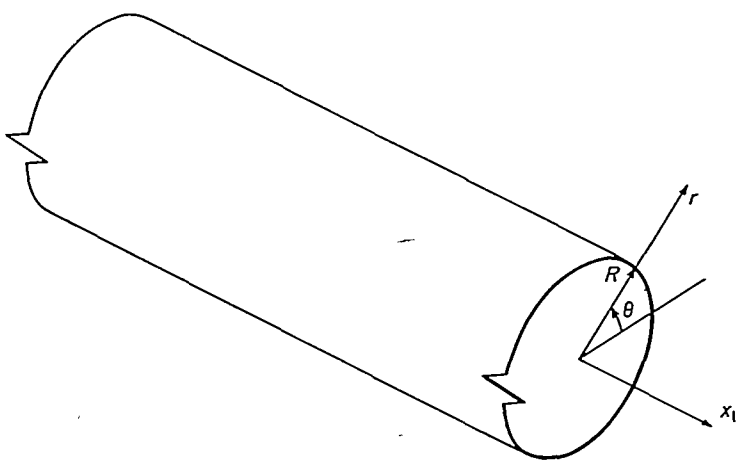

FIGURE 8.—Cylindrical coordinates for analysis of flow past stationary, deformed cylinder.

and, for subsonic flow ($|M_1|<1$), has the solution

$$f(r)=AI_n(|\nu|\sqrt{1-M_1^2}r)+BK_n(|\nu|\sqrt{1-M_1^2}r) \tag{A6}$$

AIR FLOW OUTSIDE CYLINDER

For air flowing over the outside of the cylinder, the formulation of the problem is completed by the specification of the boundary condition

$$\phi_r(x_1,R,\theta)=M_1cw_{x_1} \tag{A7}$$

at the cylinder wall and the proper conditions at infinity.

By use of equations (A1) and (A3), equation (A7) becomes

$$f_r(R)=-iM_1c\nu\overline{w} \tag{A8}$$

The resulting pressure perturbation Δp can be calculated from the linearized Bernoulli's equation

$$\Delta p(x_1,r,\theta)=-\rho M_1c\phi_{x_1} \tag{A9}$$

and is

$$\Delta p(x_1,r,\theta)=\rho M_1c\mathrm{Re}(if\nu e^{-i\nu x_1}\cos n\theta) \tag{A10}$$

Supersonic flow.—For supersonic flow, the Sommerfeld condition (that is, that there be no incoming disturbances from infinity) requires that, for large values of r, the velocity potential ϕ be essentially a function of $x_1-\beta r$ for $M_1>0$ and a function of $x_1+\beta r$ for $M_1<0$ (where $\beta=\sqrt{M_1^2-1}$). Then, from the relation for ϕ (eq. (A3)), it is apparent that, for large values of r, $f(r)$ must behave like $e^{i\frac{M_1}{|M_1|}\beta\nu r}$. Substituting the asymptotic approximations (ref. 14)

$$\left.\begin{aligned}H_n^{(1)}(z)&\sim\sqrt{\frac{2}{\pi z}}\,e^{i\left[z-\left(n+\frac{1}{2}\right)\frac{\pi}{2}\right]}\\ H_n^{(2)}(z)&\sim\sqrt{\frac{2}{\pi z}}\,e^{-i\left[z-\left(n+\frac{1}{2}\right)\frac{\pi}{2}\right]}\end{aligned}\right\} \tag{A11}$$

into equation (A5) gives, for large values of r,

$$f(r)\sim\sqrt{\frac{2}{\pi|\nu|\beta r}}\left[e^{-i\left(n+\frac{1}{2}\right)\frac{\pi}{2}}Ae^{i|\nu|\beta r}+e^{i\left(n+\frac{1}{2}\right)\frac{\pi}{2}}Be^{-i|\nu|\beta r}\right] \tag{A12}$$

Hence, the Sommerfeld condition requires that $B=0$ for $M_1\nu>0$ and $A=0$ for $M_1\nu<0$. Therefore, equation (A5) becomes

$$f(r)=AH_n^{(j)}(|\nu|\sqrt{M_1^2-1}r)\qquad\left(j=\begin{cases}1 \text{ for } M_1\nu>0\\ 2 \text{ for } M_1\nu<0\end{cases}\right) \tag{A13}$$

If, now, A is evaluated by use of the boundary condition, equation (A8), and the resulting expression for f is substituted into equation (A10), the perturbation pressure on the cylinder wall is obtained as

$$\Delta p(x_1,R,\theta)=\rho c^2 \mathrm{Re}\left[R\nu^2 M_1^2 \frac{H_n^{(j)}(z)}{zH_n^{(j)\prime}(z)}\overline{w}e^{-i\nu x_1}\cos n\theta\right] \quad \left(j=\begin{cases}1 \text{ for } M_1\nu>0\\ 2 \text{ for } M_1\nu<0\end{cases}\right) \tag{A14}$$

where

$$z=R|\nu|\sqrt{M_1^2-1}$$

Subsonic flow.—For subsonic flow over the outside of the cylinder, the potential must remain finite at infinity; hence, equation (A6) reduces to

$$f(r)=BK_n(|\nu|\sqrt{1-M_1^2}r) \tag{A15}$$

If B is evaluated by using the boundary condition, equation (A8), and the resulting expression for f is then substituted into equation (A10), the resulting perturbation pressure on the cylinder wall is

$$\Delta p(x_1,R,\theta)=\rho c^2 \mathrm{Re}\left[R\nu^2 M_1^2 \frac{K_n(\zeta)}{\zeta K_n'(\zeta)}\overline{w}e^{-i\nu x_1}\cos n\theta\right] \tag{A16}$$

where $\zeta=R|\nu|\sqrt{1-M_1^2}$.

FLUID FLOW INSIDE CYLINDER

It is assumed that the fluid inside the cylinder may be other than air and may exist under different conditions from the air outside the cylinder. Thus, the boundary condition at the cylinder wall is

$$f_r(R)=-iM_1c_i\nu\overline{w} \tag{A17}$$

and Bernoulli's equation may be written as

$$\Delta p_i(x_1,r,\theta)=\rho_i M_1 c_i \mathrm{Re}(if\nu e^{-i\nu x_1}\cos n\theta) \tag{A18}$$

where the subscript i refers to the properties of the fluid inside the cylinder.

For either supersonic or subsonic flow, the velocity potential must remain finite throughout the cylinder. If this requirement is to be met at $r=0$, the solutions given by equations (A5) and (A6) must reduce, respectively, to

$$f(r)=AJ_n(|\nu|\sqrt{M_1^2-1}\,r) \tag{A19}$$

and

$$f(r)=AI_n(|\nu|\sqrt{1-M_1^2}\,r) \tag{A20}$$

With the constant A determined through the use of the boundary condition, equation (A17), and the resulting expressions for f substituted into equation (A18), the perturbation pressure for $|M_1|>1$ becomes

$$\Delta p_i(x_1,R,\theta)=\rho_i c_i^2 \mathrm{Re}\left[R\nu^2 M_1^2 \frac{J_n(z)}{zJ_n'(z)}\overline{w}e^{-i\nu x_1}\cos n\theta\right] \tag{A21}$$

and, for $|M_1|<1$,

$$\Delta p_i(x_1,R,\theta)=\rho_i c_i^2 \mathrm{Re}\left[R\nu^2 M_1^2 \frac{I_n(\zeta)}{\zeta I_n'(\zeta)}\overline{w}e^{-i\nu x_1}\cos n\theta\right] \tag{A22}$$

These results hold for flow in either direction. Note that, for these air forces, the pressure is always in phase with the motion.

APPENDIX B

AIR FORCES ON A CYLINDER IN DIVERGENT OSCILLATION

The outward lift force on a cylinder wall executing the simple harmonic motion (ω real)

$$w(x,\theta,t)=\mathrm{Re}(\overline{w}e^{-i\nu x}e^{i\omega t}\cos n\theta) \tag{B1}$$

in the presence of moving air outside and a stationary fluid inside the cylinder has been determined. (See eqs. (3) to (6).) The amplitude of this force is expressed by

$$\bar{l}=-\rho c^2F\left(M-\frac{\omega}{\nu c},R\nu,n\right)+\rho_i c_i^2F_i\left(\frac{\omega}{\nu c_i},R\nu,n\right) \tag{B2}$$

In equation (B2),

$$\left.\begin{aligned}F(\xi,R\nu,n)&=\xi^2\frac{K_n(\zeta)}{\zeta K_n'(\zeta)} && (|\xi|<1)\\ &=\xi^2\frac{H_n^{(j)}(z)}{zH_n^{(j)\prime}(z)}\quad\left(j=\begin{cases}1\text{ for }R\nu\xi>0\\2\text{ for }R\nu\xi<0\end{cases}\right) && (|\xi|>1)\end{aligned}\right\} \tag{B3}$$

and

$$\left.\begin{aligned}F_i(\xi,R\nu,n)&=\xi^2\frac{I_n(\zeta)}{\zeta I_n'(\zeta)} && (|\xi|<1)\\ &=\xi^2\frac{J_n(z)}{zJ_n'(z)} && (|\xi|>1)\end{aligned}\right\} \tag{B4}$$

where

$$\zeta=R|\nu|\sqrt{1-\xi^2}$$

$$z=R|\nu|\sqrt{\xi^2-1}$$

It is desired to extend these air-force functions to apply to divergent motion of the cylinder (ω complex with a negative imaginary part). This extension can be made by using analytic continuation; in fact, it can be shown by Fourier transform analysis that the necessary and sufficient conditions for the extensibility of the air-force functions to divergent motion are that the air-force functions possess analytic continuations which have no singularities anywhere in the unstable half-plane ($\mathrm{Im}(\omega)<0$) and reduce smoothly to equations (B3) and (B4) on the real axis. Singularities may possibly exist along the real axis, but the real axis is specifically excluded from the unstable half-plane.

Consider the function $F(\xi,R\nu,n)$. Examination of the manner in which ω appears in F (see eq. (B2)) shows that the unstable half of the ξ-plane is the upper half-plane if ν is positive and the lower half-plane if ν is negative. It can be verified that the desired analytic continuation of F into the proper half-plane is given as follows:

$$F(\xi,R\nu,n)=\frac{\xi^2K_n(R|\nu|\sqrt{1-\xi^2})}{R|\nu|\sqrt{1-\xi^2}\,K_n'(R|\nu|\sqrt{1-\xi^2})} \tag{B5}$$

where the desired branch of the multiple-valued function F is the one for which the cuts are as shown in sketch 6:

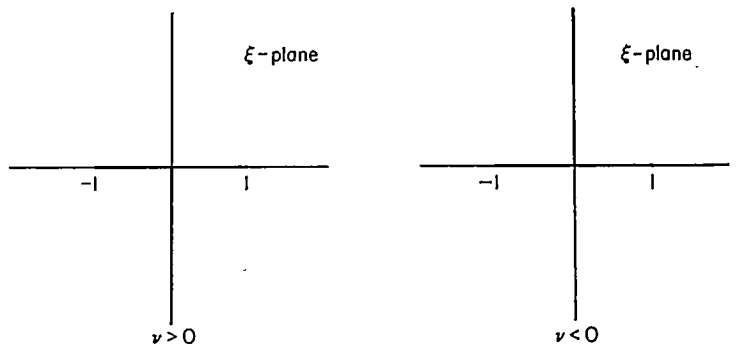

Sketch 6.

and

$$\left.\begin{aligned}F(\sqrt{2},R\nu,n)&=\frac{2H_n^{(1)}(R|\nu|)}{R|\nu|H_n^{(1)\prime}(R|\nu|)} && (\nu>0)\\ &=\frac{2H_n^{(2)}(R|\nu|)}{R|\nu|H_n^{(2)\prime}(R|\nu|)} && (\nu<0)\end{aligned}\right\} \tag{B6}$$

As $\mathrm{Im}(\xi)$ approaches zero from the proper direction, the definitions given by equations (B3) result. Furthermore, no branch points or cuts of the function F occur in the unstable half of the ξ-plane, and, in addition, Nyquist diagram techniques can be employed to show that there are no poles of F in this region.

In a similar manner, the analytic continuation of F_i can be expressed in the form

$$F_i(\xi,R\nu,n)=\frac{\xi^2I_n(R|\nu|\sqrt{1-\xi^2})}{R|\nu|\sqrt{1-\xi^2}\,I_n'(R|\nu|\sqrt{1-\xi^2})} \tag{B7}$$

No difficulties with branch points occur for F_i; the functions I_n and I_n' are entire functions and the combination I_n/zI_n' is an even function. Therefore, F_i is inherently a single-valued function of ξ.

The air forces used in the analysis of the ring-stiffened cylinder can be similarly written for divergent motion. For $m\neq0$, it is only necessary to replace ν by $m\pi/a$ in equations (B5) to (B7). For $m=0$, it is necessary to specify the air forces separately. Thus, for divergent motion (see eqs. (33) to (35)),

$$l_0=-\rho c^2G(k,\alpha,n)+\rho_i c_i^2G_i\left(\frac{c}{c_i}k,\alpha,n\right) \tag{B8}$$

where

$$G(\xi,\alpha,n)=\frac{\xi H_n^{(2)}(\alpha\xi)}{\alpha H_n^{(2)\prime}(\alpha\xi)} \tag{B9}$$

$$G_i(\xi,\alpha,n)=\frac{\xi J_n(\alpha\xi)}{\alpha J_n'(\alpha\xi)} \tag{B10}$$

The desired branch of the multiple-valued function G is the one for which the cut extends from the origin to infinity along the positive imaginary axis and

$$G(1,n,\alpha)=\frac{H_n^{(2)}(\alpha)}{\alpha H_n^{(2)\prime}(\alpha)} \tag{B11}$$

APPENDIX C

EQUILIBRIUM OF UNSTIFFENED CYLINDER—FLÜGGE'S EQUATION

The simplifying assumptions used in deriving Donnell's differential equation (eq. (7)) result in a loss of accuracy when the condition $n^2>>1$ is violated; further, terms which become important when the longitudinal wave lengths become large (that is, when the behavior of a cylinder approaches that of a ring) have been omitted.

The more complicated theory proposed by Flügge (see, for example, ref. 11) is not characterized by either of these limitations. Flügge's equations may be written in the form of a single equation in w, which, for $(h/R)^2<<1$ reduces (see refs. 11 and 12) to

$$D\left\{\nabla^4 w+\frac{1}{R^4}\nabla^{-4}\left[\frac{12(1-\mu^2)}{(h/R)^2}w_{xxxx}+\frac{2(2-\mu)}{R^2}w_{xx\theta\theta}+\frac{1}{R^4}w_{\theta\theta\theta\theta}+2\mu R^2 w_{xxxxxx}+6w_{xxxx\theta\theta}+\frac{2(4-\mu)}{R^2}w_{xx\theta\theta\theta\theta}+\frac{2}{R^4}w_{\theta\theta\theta\theta\theta\theta}\right]\right\}+\rho_s h w_{tt}=l \tag{C1}$$

where imposed midplane stresses have not been included. As in Donnell's equation, equation (C1) takes no account of inertia forces in the longitudinal and circumferential directions.

Substitution of w and l for the unstiffened cylinder (eqs. (1), (3), and (4)) into equation (C1) gives

$$\frac{\rho_s}{\rho}\frac{h}{R}(k^2-\Omega^2)+\frac{\rho_i}{\rho}\left(\frac{c_i}{c}\right)^2 F_i\left(\frac{c}{c_i}k,\bar{\nu},n\right)-F(M-k,\bar{\nu},n)-i\frac{\bar{\nu}}{|\bar{\nu}|}\epsilon k=0 \tag{C2}$$

where the term $-i\frac{\bar{\nu}}{|\bar{\nu}|}\epsilon k$ has been added to include qualitatively the effects of Sezawa (viscous) damping and where, now,

$$\Omega=\frac{\frac{c_s}{c}\frac{h}{R}}{\sqrt{12(1-\mu^2)}}\sqrt{\bar{\nu}^2\left(1+\frac{n^2}{\bar{\nu}^2}\right)^2+\frac{1}{\bar{\nu}^2\left(1+\frac{n^2}{\bar{\nu}^2}\right)^2}\left\{\frac{12(1-\mu^2)}{\left(\frac{h}{R}\right)^2}+2(2-\mu)\left(\frac{n}{\bar{\nu}}\right)^2+\left(\frac{n}{\bar{\nu}}\right)^4-\bar{\nu}^2\left[2\mu+6\left(\frac{n}{\bar{\nu}}\right)^2+2(4-\mu)\left(\frac{n}{\bar{\nu}}\right)^4+2\left(\frac{n}{\bar{\nu}}\right)^6\right]\right\}} \tag{C3}$$

Equation (C2) is precisely equation (8); hence, the flutter boundary in the supersonic range for the empty, unstressed cylinder is still defined by

$$M=1+\sqrt{\Omega^2-\frac{1}{n\frac{\rho_s}{\rho}\frac{h}{R}}} \tag{C4}$$

but with Ω given by the more complicated function, equation (C3). As before, the critical boundary corresponds to the minimum value of M as $\bar{\nu}$ and n are varied. Setting $\partial\Omega^2/\partial\bar{\nu}=0$ yields

$$\bar{\nu}^{10}+3n^2\bar{\nu}^8+\left[2n^4+2(3-2\mu)n^2-\frac{12(1-\mu^2)}{\left(\frac{h}{R}\right)^2}\right]\bar{\nu}^6-n^2\left[2n^4-2(5-2\mu)n^2+4(2-\mu)-\frac{12(1-\mu^2)}{\left(\frac{h}{R}\right)^2}\right]\bar{\nu}^4-3n^4(n^2-1)^2\bar{\nu}^2-n^6(n^2-1)^2=0 \tag{C5}$$

Careful examination of equation (C5) indicates that, for small values of h/R, there are two minimums of Ω^2 with an intervening maximum. Computations have been made for an aluminum cylinder at sea level by letting $n=2$, 3, and 4; both the minimums of Ω^2 were checked and, through equation (C4), the boundaries corresponding to the lower of these were determined. These results are shown by the dashed curves in figure 4; in addition, the corresponding wave lengths are given in figure 5.

APPENDIX D

IMPORTANCE OF DAMPING IN UNSTIFFENED CYLINDER

It is of interest to examine some of the results of an analysis of the empty, unstiffened cylinder which takes no account of damping (as opposed to the analysis in the body of this report which treats a cylinder in the limit as damping approaches zero). The equilibrium condition, equation (9), reduces to

$$\bar{L}\equiv\frac{\rho_s}{\rho}\frac{h}{R}(k^2-\Omega^2)-F(M-k,\bar{\nu},n)=0 \tag{D1}$$

and its constituent functions vary as in figure 2 except that now $\mathrm{Im}(\bar{L})\equiv 0$ throughout the range $M-1<k<M+1$.

A typical Nyquist diagram (resulting when k traverses the path of fig. 3) is shown in sketch 7 which corresponds

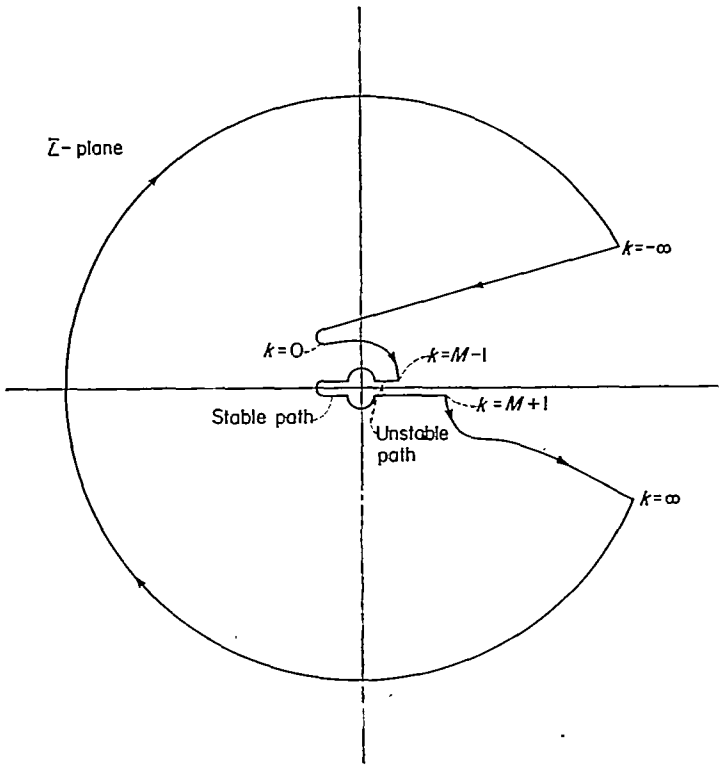

Sketch 7.

to the particular conditions $\bar{\nu}>0$, $0<M-1<\Omega<M$, $\mathrm{Re}(\bar{L})_{k=M-1}>0$, and $\mathrm{Re}(\partial\bar{L}/\partial k)_{k=M-1}<0$. (The infinitesimal, counterclockwise semicircles correspond to infinitesimal, counterclockwise semicircles traversed by k to exclude zeros of $\bar{L}$ on the real axis from the lower half-plane.) These particular conditions are illustrated because they show clearly the possible existence of a stable condition with $\mathrm{Re}(\bar{L})_{k=M-1}>0$, a circumstance found impossible with damping present. The reason for the difference, of course, is that, for $k>0$, the damping term is a negative imaginary quantity and even the smallest amount of damping shifts all the portion of the diagram corresponding to the range $M-1<k<M+1$ below the real axis.

Note that, for the case of zero damping, satisfaction of equilibrium ($\bar{L}=0$) with k real is not always sufficient for definition of the boundary; for the conditions in the cited example, the roots of $\bar{L}=0$ do not pass directly from the upper into the lower half of the k-plane as the other parameters are varied, but linger awhile on the real axis. Instability occurs when a root leaves the real axis and enters the lower half of the k-plane. For the cited example, this definition corresponds to the simultaneous solution of the equations

$$\left.\begin{aligned}\bar{L}&=0\\ \frac{\partial\bar{L}}{\partial k}&=0\end{aligned}\right\} \tag{D2}$$

in the range $M-1<k<M$.

Another significant difference in the two analyses is that, when damping is ignored, the instability in the subsonic region is low-frequency flutter and no purely static instability of the cylinder is possible. Similar differences would be found for the fluid-filled cylinder if the damping were ignored. The fact that the two assumptions, $\epsilon\rightarrow 0$ and $\epsilon\equiv 0$, produce such discontinuously different results testifies to the importance of the presence of damping in the unstiffened cylinder.

REFERENCES

1. Isaacs, R. P.: Transtability Flutter of Supersonic Aircraft Panels. U. S. Air Force Project RAND P-101, The Rand Corp., July 1, 1949.
2. Hayes, W.: A Buckled Plate in a Supersonic Stream. Rep. No. AL-1029, North American Aviation, Inc., May 10, 1950.
3. Miles, John W.: Dynamic Chordwise Stability at Supersonic Speeds. Rep. No. AL-1140, North American Aviation, Inc., Oct. 18, 1950.
4. Shen, S. F.: Flutter of a Two-Dimensional Simply-Supported Uniform Panel in a Supersonic Stream. Contract No. N5ori-07833, Office of Naval Res., Dept. Aero. Eng., M.I.T., Aug. 6, 1952.
5. Sylvester, Maurice A., and Baker, John E.: Some Experimental Studies of Panel Flutter at Mach number 1.3. NACA TN 3914, 1956. (Supersedes NACA RM L52I16.)
6. Goland, Martin, and Luke, Yudell L.: An Exact Linear Solution for Two-Dimensional Linear Panel Flutter at Supersonic Speeds. Jour. Aero. Sci. (Readers' Forum), vol. 21, no. 4, Apr. 1954, pp. 275–276.

7. Hedgepeth, John M., Budiansky, Bernard, and Leonard, Robert W.: Analysis of Flutter in Compressible Flow of a Panel on Many Supports. Jour. Aero. Sci., vol. 21, no. 7, July 1954, pp. 475–486.
8. Nelson, Herbert C., and Cunningham, Herbert J.: Theoretical Investigation of Flutter of Two-Dimensional Flat Panels With One Surface Exposed to Supersonic Potential Flow. NACA Rep. 1280, 1956. (Supersedes NACA TN 3465.)
9. Fung, Y. C.: The Flutter of a Buckled Plate in Supersonic Flow. GALCIT Rep. No. OSR–TN–55–237, July 1955.
10. Donnell, L. H.: Stability of Thin-Walled Tubes Under Torsion. NACA Rep. 479, 1933.
11. Kempner, Joseph: Remarks on Donnell's Equations. Jour. Appl. Mech., vol. 22, no. 1, Mar. 1955, pp. 117–118.
12. Hoff, N. J.: The Accuracy of Donnell's Equations. Jour. Appl. Mech., vol. 22, no. 3, Sept. 1955, pp. 329–334.
13. Junger, Miguel C.: The Physical Interpretation of the Expression for an Outgoing Wave in Cylindrical Coordinates. Jour. Acous. Soc. of America, vol. 25, no. 1, Jan. 1953, pp. 40–47.
14. McLachlan, N. W.: Bessel Functions for Engineers. Clarendon Press (Oxford), 1934.
15. Jahnke, Eugene, and Emde, Fritz: Tables of Functions. Fourth ed., Dover Publications, 1945.
16. Batdorf, S. B.: A Simplified Method of Elastic-Stability Analysis for Thin Cylindrical Shells. NACA Rep. 874, 1947. (Formerly included in NACA TN'S 1341 and 1342.)